

Elastic and inelastic tunneling in a strained-layer double-barrier resonant-tunneling structure

W. I. E. Tagg

Department of Physics, University of Sheffield, Sheffield S3 7RH, United Kingdom

C. R. H. White*

Department of Physics, University of Nottingham, Nottingham NG7 2RD, United Kingdom

M. S. Skolnick

Department of Physics, University of Sheffield, Sheffield S3 7RH, United Kingdom

L. Eaves

Department of Physics, University of Nottingham, Nottingham NG7 2RD, United Kingdom

M. T. Emeny and C. R. Whitehouse

Defence Research Agency, Saint Andrew's Road, Malvern, Worcestershire WR14 3PS, United Kingdom

(Received 8 February 1993)

A magnetotransport study of the tunneling processes in a double-barrier resonant-tunneling structure (DBRTS) containing a narrower gap strained-layer quantum-well region is reported. Clear evidence for the occurrence of both elastic and inelastic tunneling as a function of applied bias is found. Analysis of the magneto-oscillations shows that the device is on resonance at $V=0$, as expected for a DBRTS with a strained $\text{In}_y\text{Ga}_{1-y}\text{As}$ quantum-well region of narrower band gap than that of the GaAs contacts. The anomalous bias voltages of the LO-phonon-assisted tunneling features are explained from the variation of charge density in the quantum well with bias, obtained from complementary optical measurements.

I. INTRODUCTION

The incorporation of a strained $\text{In}_y\text{Ga}_{1-y}\text{As}$ layer in the quantum-well (QW) region of a $\text{GaAs-Al}_x\text{Ga}_{1-x}\text{As}$ based double-barrier resonant-tunneling structure (DBRTS) can have a profound effect on the tunneling and current-voltage (I - V) characteristics of the device.¹⁻⁴ The addition of indium to GaAs results in a narrowing of the fundamental band gap by 100 meV for the indium composition of 0.09 discussed in the present work.⁵ The narrower band gap of the quantum well relative to the GaAs contact regions can lead to charge transfer from the contacts into the QW in order to establish equilibrium at zero applied bias (V).^{2,4} When this occurs the device will be on resonance at $V=0$,⁴ in strong contrast to conventional $\text{GaAs-Al}_x\text{Ga}_{1-x}\text{As-GaAs-Al}_x\text{Ga}_{1-x}\text{As-GaAs}$ structures where finite bias must be applied before resonant tunneling can arise. Furthermore, since the resonance condition is achieved at $V=0$, at low biases the tunneling will have the character expected from three-dimensional (3D) emitter⁶⁻⁸ states into the two-dimensional (2D) QW level. This is the case even for the relatively low doped GaAs contact layers close to the $\text{Al}_x\text{Ga}_{1-x}\text{As}$ barriers required to achieve high-quality tunnel barriers with minimal perturbation from the dopant atoms. It is only at higher applied bias, as accumulation of electrons at the emitter barrier becomes more significant, that the tunneling process will acquire the character expected from 2D (emitter) to 2D QW states.

The present paper reports a magnetotransport study of

the tunneling processes in such a $\text{GaAs-Al}_x\text{Ga}_{1-x}\text{As-In}_y\text{Ga}_{1-y}\text{As-Al}_x\text{Ga}_{1-x}\text{As-GaAs}$ DBRTS. Magneto-oscillations, periodic in $1/B$, are observed in the tunnel current over a wide range of applied bias.⁷⁻¹² These oscillations arise from two distinct types of physical effects associated with elastic and inelastic tunneling processes. At low bias, in the region of the first tunneling resonance, the tunneling is shown to be elastic in character. As soon as the energy separation ($E_F - E_1$) between the quasi-Fermi-level (E_F) in the emitter and the first confined state (E_1) in the QW is equal to a longitudinal-optical (LO) phonon energy, the tunneling becomes inelastic with emission of a GaAs-like LO phonon in the tunneling process. In addition, clear evidence for tunneling with non-conservation of lateral momentum (k_1) is presented. Comparison of the energy separation deduced at low bias with the total applied bias shows that most of the additional voltage applied between the peak of the first resonance and the onset of inelastic tunneling is dropped across the emitter region, in strong contrast to the situation in conventional GaAs based structures. This behavior in the strained $\text{In}_y\text{Ga}_{1-y}\text{As}$ layer structures is shown to be a consequence of the finite charge in the QW at $V=0$.

II. EXPERIMENTAL DETAILS

The experiments were carried out on a symmetric $\text{GaAs-Al}_{0.33}\text{Ga}_{0.67}\text{As-In}_{0.09}\text{Ga}_{0.91}\text{As-Al}_{0.33}\text{Ga}_{0.67}\text{As-GaAs}$ DBRTS grown by molecular-beam epitaxy at 530°C. The details of the structure are given in Table I.

All of the measurements were taken at 4.2 K, on a 200- μm -diam mesa, with the device illuminated with an estimated 0.1 W/cm² light from a He-Ne laser (1.96 eV). Optical access was made via a fiber optic. The illumination conditions were adjusted to be very similar to those employed for the photoluminescence (PL) and photoluminescence excitation (PLE) studies of Ref. 4, in order to permit direct comparison of the optical and magneto-transport results. Magnetic fields from $B=0$ to 11 T, parallel to current flow in the device, were applied using a superconducting solenoid.

III. RESULTS AND DISCUSSION

The experimental I - V characteristic is shown in Fig. 1(a). Two resonances are observed with peaks at 0.012 and 0.7–0.8 V, corresponding to tunneling into E_1 and E_2 , the two quasiconfined electron levels in the well. From zero bias, the application of a small bias causes an immediate rise in current which continues until the first resonant peak has been reached at 0.012 V. Beyond the peak of the first resonance two features, labeled LO_1 and

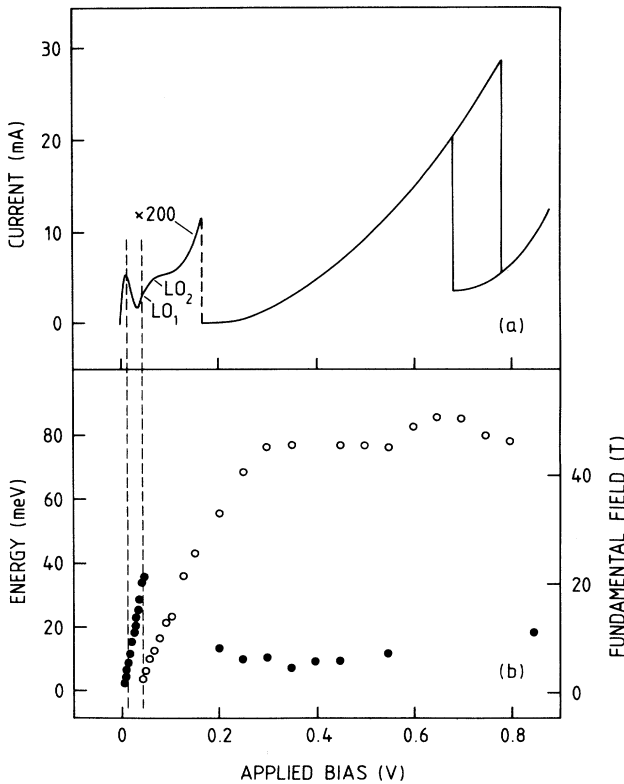


FIG. 1. (a) Device current against applied bias. The LO-phonon-assisted tunneling features LO_1 and LO_2 are indicated. The dashed vertical lines are guides to the eye and indicate the bias positions of first resonance and LO_1 tunneling feature, respectively. (b) Fundamental field (right-hand axis) and energy difference (left-hand axis) deduced from magneto-oscillations as a function of bias. The elastic tunneling results from 0 to 0.042 V are indicated by filled circles, and the inelastic tunneling results by open circles.

TABLE I. Composition of alloy layers, doping of GaAs regions, and layer thicknesses. All alloys regions are nominally undoped.

Material	Composition doping	Thickness (\AA)
GaAs n -type contact	$1 \times 10^{18} \text{ cm}^{-3}$	9000
GaAs n type	$2 \times 10^{17} \text{ cm}^{-3}$	1000
GaAs	undoped	100
$\text{Al}_x\text{Ga}_{1-x}\text{As}$	$x=0.33$	85
GaAs	undoped	10
$\text{In}_y\text{Ga}_{1-y}\text{As}$	$y=0.09$	75
GaAs	undoped	10
$\text{Al}_x\text{Ga}_{1-x}\text{As}$	$x=0.33$	85
GaAs	undoped	100
GaAs n type	$2 \times 10^{17} \text{ cm}^{-3}$	1000
GaAs n -type contact	$1 \times 10^{18} \text{ cm}^{-3}$	9000
GaAs n -type substrate	$1 \times 10^{18} \text{ cm}^{-3}$	

LO_2 , respectively, are observed. These are due to LO-phonon-assisted inelastic tunneling and occur at 0.045 and 0.07 V. Beyond 0.7 V, the current rises to the second resonance at 0.7–0.8 V, which shows marked bistability.

The form of the I - V characteristic can be understood by considering the band structure of the device. Since the $\text{In}_y\text{Ga}_{1-y}\text{As}$ band gap is smaller than that of GaAs, at zero bias charge will flow from the n^+ -type GaAs contacts into the well to establish equilibrium. This charge was deduced to be $1 \times 10^{11} \text{ cm}^{-2}$ at $V=0$ from the PL and PLE measurements of Ref. 4. The equilibrium-band diagram of the DBRTS at zero bias, Fig. 2, shows the

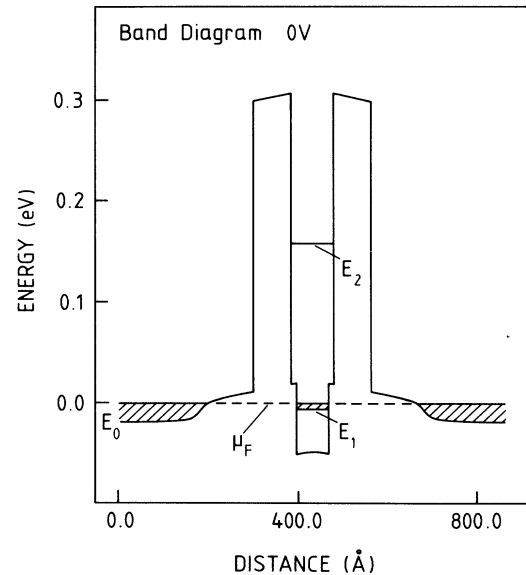


FIG. 2. Zero-bias band diagram, of strained-layer double-barrier resonant-tunneling structure, obtained from self-consistent Hartree calculations. The band bending arises from charge transfer of $1 \times 10^{11} \text{ cm}^{-2}$ into the quantum well from the doped contact regions to establish equilibrium. The zero of energy is defined as the bottom of the conduction band in the GaAs contacts far from the double-barrier region. The dashed line shows the position of the electron Fermi level μ_F .

effect of this charge movement. The band diagram was calculated using a self-consistent solution to Poisson's and Schrödinger's equations as described in Ref. 4.

Following the charge transfer the lowest well level (E_1) is at the same energy as the filled emitter levels and so the device is on resonance.⁴ The application of a small bias causes resonant tunneling to occur, as demonstrated by the finite slope of the I - V characteristic at zero bias. Electrons tunnel from the 3D conduction-band states in the emitter into the 2D QW state E_1 . The first resonant-tunneling peak occurs when E_1 is at the same energy as the bottom of the conduction band in the emitter, E_c .⁶

The variation of current, as a function of applied magnetic field, was recorded for a wide range of biases. A selection of the results is shown in Fig. 3. The oscillations shown result from the Landau quantization of the transverse kinetic energy of the electron states in the emitter and the quantum well. In magnetic field the energy levels of electrons in the emitter and the quantum well are given by

$$E = E_c + (n + \frac{1}{2})\hbar\omega_c + \hbar^2 k_z^2 / 2m^* \quad (3D \text{ emitter}), \quad (1)$$

$$E = E_0 + (n + \frac{1}{2})\hbar\omega_c \quad (2D \text{ emitter}), \quad (2)$$

$$E = E_1(V) + (n' + \frac{1}{2})\hbar\omega_c \quad (\text{quantum well}), \quad (3)$$

where n and n' are Landau-level (LL) quantum numbers, $\omega_c = eB/m^*$, E_0 is the lowest-energy populated state in the emitter when accumulation is significant, and k_z is the electron wave vector in the tunneling direction. The effective-mass values in the QW and emitter regions are expected to differ by less than 5%, and so the same values of m^* ($0.07m_0$), and hence ω_c , are employed in Eqs. (1)–(3).¹³

At low bias when the potential drop across the emitter region is of the order of or less than the Fermi energy in the GaAs contacts, the tunneling will have 3D (emitter) to 2D (well) character. For elastic tunneling, with conservation of k_{\perp} the electrons which can tunnel into the QW state with energy E_1 are those which have transverse kinetic energies between E_1 and E_F .^{6,7} Since the transverse kinetic energy is quantized into LL's, oscillations in the tunnel current are expected whenever $(n + \frac{1}{2})\hbar\omega_c = E_F - E_1$, resulting in oscillations periodic in $1/B$ with fundamental field $B_f = m^*/e\hbar(E_F - E_1)$.^{7,8,11,12} Analysis of the oscillations of Fig. 3 thus gives the energy separation of emitter and QW states as a function of applied bias. The variation of the B_f results, and hence emitter to QW energy separation, is plotted in Fig. 1(b).

At higher biases ($\gtrsim 100$ mV), when the voltage drop across the GaAs emitter region is greater than E_F (11 meV) in the contacts, carrier accumulation in the emitter contact will become more important and the tunneling will acquire greater 2D to 2D character. 2D to 2D tunneling occurs when Landau levels in the emitter accumulation layer are resonant with those in the well, when

$$E_0 - E_1 = (n - n')\hbar eB/m^* + i\hbar\omega_{LO}. \quad (4)$$

Tunneling with $n = n'$ corresponds to the conservation of k_{\perp} at $B=0$. When $n \neq n'$, k_{\perp} is not conserved. The $i\hbar\omega_{LO}$ term represents the possible emission of a LO phonon. For elastic scattering, $i=0$. In the case of inelastic scattering, a phonon is emitted and $i=1$. From Eq. (4), magneto-oscillations with fundamental field $B_f = m^*/e\hbar(E_0 - E_1 - i\hbar\omega_{LO})$ are then expected.

Throughout the bias range 0–0.012 V [the filled circles in Fig. 1(a)] the tunneling is expected to be 3D to 2D and elastic, and so the B_f results give the energy difference $E_F - E_1$. From Fig. 1(b), $E_F - E_1$ found at the first resonance [the first vertical dashed line is drawn as a guide to the eye between Figs. 1(a) and 1(b)] is 11 meV ($B_f = 5.6$ T). The level E_1 then lies at an energy corresponding to the bottom of the distribution of the 3D emitter electrons.^{6,7} Thus, the Fermi energy in the emitter, $E_F - E_c$ is deduced to be 11 meV,¹⁴ corresponding to doping of $1 \times 10^{17} \text{ cm}^{-3}$, in reasonable agreement with the nominal value of $2 \times 10^{17} \text{ cm}^{-3}$.

The observation of magneto-oscillations at very low biases with the B_f value increasing strongly with bias is consistent with the device being on resonance at $V=0$. Oscillations with B_f of 2.4 T, corresponding to $E_F - E_1 = 4$ meV are observed at the smallest applied bias

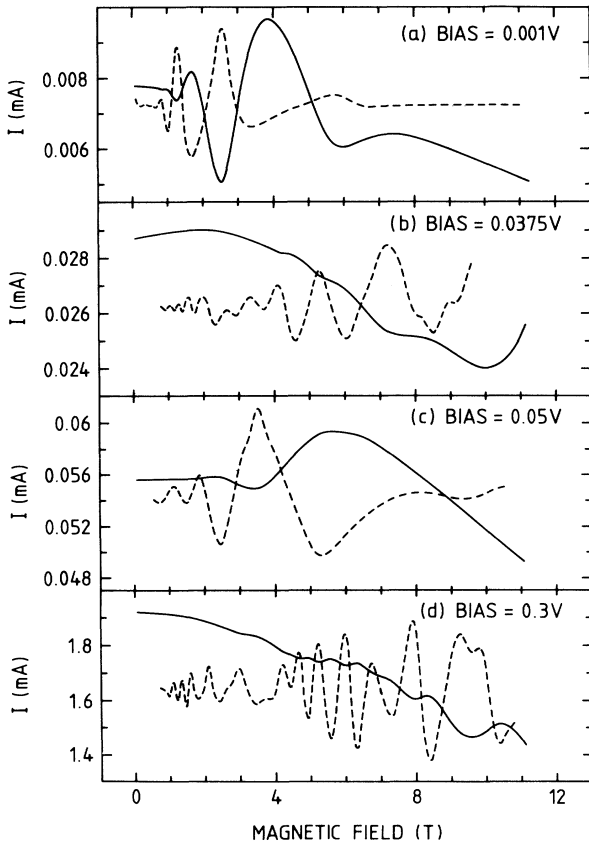


FIG. 3. I - B (solid line) and $d^2I/d^2B - B$ (dashed line) characteristics are shown for (a) 0.001 V, (b) 0.0375 V, (c) 0.05 V, and (d) 0.3 V applied bias. In (b) two series can be seen in the $d^2I/d^2B - B$ characteristic, showing the transition between elastic and nonelastic tunneling.

studied of 1 mV. This observation of $E_F - E_1 > V_{\text{applied}}$ is consistent with the finite electron density in the well of 10^{11} cm^{-2} (equivalent to a QW Fermi energy of 3.1 meV) at $V=0$ deduced from the optical measurements of Ref. 4. Similar observations of magneto-oscillations at low bias have been reported in Refs. 11 and 15, although in these cases the devices were on resonance at $V=0$ due to the inadvertent space charge in the barriers.

From the first resonant-tunneling peak at 0.012 V to the LO-phonon-assisted tunneling feature at 0.042 V, the B_f results of Fig. 1(b) are continuous with those of the first region; elastic tunneling is still observed but with the nonconservation of k_{\perp} since E_1 has dropped below the lowest-energy state of the emitter electrons, E_c .⁶ As soon as the bias is increased to the LO₁ peak at 0.042 V (the second dashed line on Fig. 1), a second series (the open circles) is observed in Fig. 1(b). The energy separation has now reached ~ 40 meV and LO-phonon-assisted tunneling can occur.

The observation of two series at the same bias in Fig. 3(b) [the filled, open circles at 0.042 V in Fig. 1(b)] with a difference in $E_F - E_1$ values of 33 meV permits the identification of the phonon mode giving rise to the LO₁ peak. The energy ($\hbar\omega_1$) of 33 meV agrees well with the expected value for the GaAs-like LO-phonon mode of the Al_{0.33}Ga_{0.67}As barrier material of 34 meV.¹⁶ It is also close to the energy of the GaAs-like LO mode in the In_{0.09}Ga_{0.91}As QW of 36 meV.¹⁷ The inelastic series first arises at a bias close to that corresponding to the first phonon shoulder, labeled LO₁ in the I - V [Fig. 1(a)], strongly reinforcing the identification of this feature as arising from LO-phonon-assisted tunneling. The LO₂ feature clearly also arises from phonon-assisted tunneling, by a LO mode of greater energy than that of the 33-meV GaAs-like phonon. The only phonon mode in the system of energy greater than 33 meV is the AlAs mode in the Al_xGa_{1-x}As barrier at 47 meV.¹⁷ Thus LO₂ is attributed to the AlAs-like mode in the barrier. The strong contribution to the I - V by a phonon mode in the tunnel barrier favors the attribution of the LO₁ ($\hbar\omega_1=33$ meV) phonon to the GaAs-like mode in the barrier, rather than in the QW.

In the bias region from 0.042 to 0.3 V the emitter states are expected to become increasingly two dimensional. In this bias range the inelastic series quickly dominates [see Fig. 3(c)] and $E_0 - E_1 - \hbar\omega_{\text{LO}}$ increases to ~ 75 meV [Fig. 1(b)] at 0.3 V. Above ~ 0.3 V, electrons begin to tunnel into the E_2 level at the onset of the second resonance of Fig. 1(a). As shown in Ref. 4 a significant fraction of the current is carried at the E_2 resonance by sequential tunneling following intersubband scattering from E_2 to E_1 . This was shown from PL spectroscopy by the detection of charge densities of approximately $(2-3) \times 10^{11} \text{ cm}^{-2}$ in E_1 while the device was biased for tunneling into E_2 .

When charge builds up in the well ($V > 0.3$ V) the electric field across the collector region will increase, with the result that the fraction of the total bias dropped across the emitter will decrease. As a result, due to the build up of charge E_0 can be "pinned" to the second well level E_F over a wide range of applied bias, as observed in Fig. 1(b)

from 0.3 to 0.8 V. Poisson equation simulations of the device, presented below, show that a value for n_s in the well of $3.8 \times 10^{11} \text{ cm}^{-2}$ at 0.7 V leads to the QW levels being at the same energy relative to the emitter levels at 0.7 V as at the onset of resonance at 0.3 V.

The results of the simulations, performed at 0.3 V, $n_s=0$; 0.7 V, $n_s=3.8 \times 10^{11} \text{ cm}^{-2}$; and 0.7 V, $n_s=0$, are shown in Figs. 4(a), 4(b), and 4(c), respectively. It is seen that the quantum-well energy level E_s is at the same energy as the emitter accumulation layer level E_0 for the two different biases of Figs. 4(a) and 4(b); the observed pinning behavior of Fig. 1(b) is explained well by the accumulation of charge in the QW with increasing bias at the second resonance. Furthermore, the required value of $n_s=3.8 \times 10^{11} \text{ cm}^{-2}$ at 0.7 V employed for Fig. 4(b) is in reasonable agreement with that obtained $[(2-3) \times 10^{11} \text{ cm}^{-2}]$ from the PL measurements of Ref. 4. When $n_s=0$ is used for the 0.7-V simulation [Fig. 4(c)], the well levels move down relative to E_0 by 80 meV. This demonstrates very clearly the effect of charge accumulation in the QW in keeping the device on resonance from 0.3 to 0.7 V, and thus leading to the pinning behavior of Fig. 1(b).

Under these pinning conditions with $E_0 = E_2$, the fun-

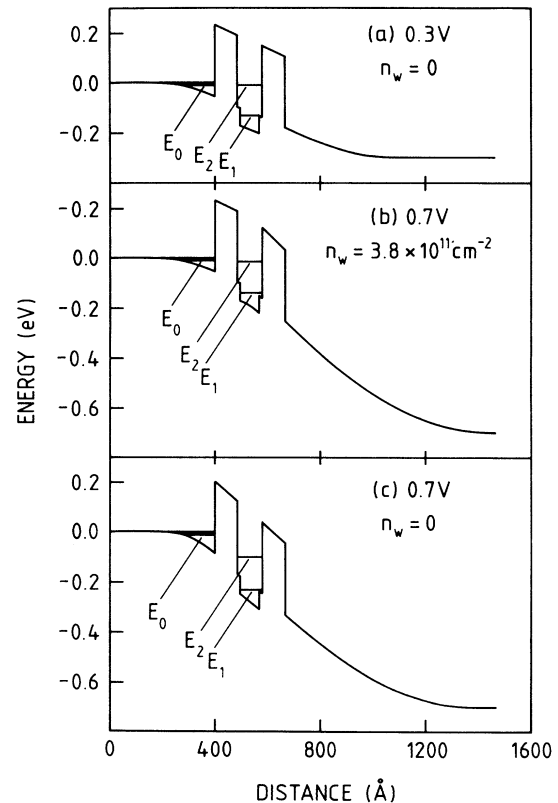


FIG. 4. Band diagrams showing the results of Poisson equation simulations for (a) 0.3 V, $n_s=0$; (b) 0.7 V, $n_s=3.8 \times 10^{11} \text{ cm}^{-2}$; and (c) 0.7 V, $n_s=0$. (a) and (b) illustrate the pinning behavior of Fig. 1(b) to be the consequence of charge buildup in the well as the resonance current increases. (c) shows that the E_2 level moves ~ 90 meV below its resonance position if charge is ejected from the well.

damental field of the magneto-oscillations will be given by $B_f = (E_2 - E_1 - \hbar\omega_{LO})m^*/\hbar e$, the oscillations arising due to modulation of the sequential tunneling current component with field.⁹ The difference in energy between the two well levels is calculated to be 119 meV. Subtracting the phonon energy of 34 meV gives 85 meV. The B_f observed in this “pinned” region in Fig. 1(b) from 0.3 to ~ 0.7 V corresponds to an energy difference of approximately 80 meV, in good agreement with the calculated $E_2 - E_1 - \hbar\omega_1$ value. In this region a second series, corresponding to an energy of approximately 10 meV, is seen. This probably arises from modulation of the series resistance of the emitter contact by 3D Shubnikov-de Haas oscillations in the emitter region away from the barriers. The E_F value of 10 meV thus deduced for the bulk emitter region is in good agreement with the 11 meV found earlier from B_f at the peak of the first resonance on the 3D-2D tunneling model.

Finally we discuss the apparently anomalous bias voltage positions of the phonon-assisted tunneling features. The LO_1 feature appears at a bias only ~ 30 meV above the first resonance. As the phonon feature appears when the level in the well has moved $\hbar\omega_1$ (33 meV) below its energetic position at the peak of the resonance, this result means that all the additional bias between the resonance peak (0.012 V) and LO_1 (0.042 V) appears across the emitter half of the device. This contrasts with the behavior of a GaAs- $Al_{0.33}Ga_{0.67}As$ -GaAs- $Al_{0.33}Ga_{0.67}As$ -GaAs device where more than half of the extra applied bias is dropped over the collector.⁷ In previous work,⁴ PLE measurements were used to monitor the changes in n_s in the well in the low bias range as the applied bias was increased from zero to ~ 0.10 V. Increasing the bias, in the range from 0 to above the phonon features, resulted in a decrease in n_s from 10^{11} cm⁻² at $V=0$ to 0.6×10^{11} cm⁻² at 0.012 V, further decreasing

to 0.45×10^{11} cm⁻² at LO_1 at 0.042 V. The finite n_s at $V=0$ arises from the charge transfer into the narrower gap QW required to establish equilibrium at $V=0$.

Based on these values of n_s , device simulations were carried out to understand the anomalous voltage separation of the resonance peak and the LO_1 feature. Holding the charge in the QW constant with bias resulted in a calculated voltage separation of 0.066 V between the resonance peak and LO_1 . The 0.066 V corresponds to the change in applied bias necessary to increase the voltage drop between emitter and QW by $\hbar\omega_1 = 34$ meV, the extra bias (0.066–0.034 mV) appearing across the collector half of the device. On the other hand, when the well charge was allowed to decrease as indicated by the PLE results, it was found that the extra applied bias needed to reach the LO_1 feature from the first resonance peak was only 0.049 V, in reasonable agreement with the observed value of 0.042–0.012=0.03 V. The physical reason for the reduction in calculated bias from 0.066 to 0.049 V is that when the charge density in the well decreases with bias, the electric field and hence voltage drop across the collector region will decrease, with the result that a greater fraction of the applied bias appears across the emitter region, as required.

IV. CONCLUSION

In conclusion, a magnetotransport study of a strained-layer DBRTS has been reported. Both elastic and inelastic contributions to the tunneling processes have been deduced from analysis of the magneto-oscillations. The anomalously low voltage separation of elastic and LO-phonon-assisted tunneling features and the pinning of emitter and QW energy levels over a wide range of bias have been well accounted for on the basis of the variation of the charge density in the QW with bias.

*Present address: STC Optical Systems, Paignton, Devon TQ4 78E, UK.

¹R. Kapre, A. Madhukar, K. Kaviani, S. Guha, and K. C. Rajkumar, *Appl. Phys. Lett.* **56**, 922 (1990).

²H. M. Yoo, S. M. Goodnick, and J. R. Arthur, *Appl. Phys. Lett.* **56**, 84 (1990).

³H. Reichert, D. Bernklau, J. P. Reithmaier, and R. D. Schnell, *Electron Lett.* **26**, 340 (1990).

⁴W. I. E. Tagg, M. S. Skolnick, M. T. Emeny, A. W. Higgs, and C. R. Whitehouse, *Phys. Rev. B* **46**, 1505 (1992).

⁵G. Ji, D. Huang, U. K. Reddy, T. S. Henderson, R. Houdré, and H. Morkoç, *J. Appl. Phys.* **62**, 3366 (1987).

⁶S. Luryi, *Appl. Phys. Lett.* **47**, 490 (1985).

⁷E. E. Mendez, L. Esaki, and W. I. Wang, *Phys. Rev. B* **33**, 2893 (1986).

⁸F. W. Sheard and G. A. Toombs, *Appl. Phys. Lett.* **52**, 1228 (1988).

⁹L. Eaves, G. A. Toombs, F. W. Sheard, C. A. Payling, M. L. Leadbeater, E. S. Alves, T. J. Foster, P. E. Simmonds, M. Henini, O. H. Hughes, J. C. Portal, G. Hill, and M. A. Pate, *Appl. Phys. Lett.* **52**, 212 (1988).

¹⁰C. A. Payling, E. S. Alves, L. Eaves, T. J. Foster, M. Henini,

O. H. Hughes, P. E. Simmonds, F. W. Sheard, and G. A. Toombs, *Surf. Sci.* **196**, 404 (1988).

¹¹M. L. Leadbeater, L. Eaves, P. E. Simmonds, G. A. Toombs, F. W. Sheard, P. A. Claxton, G. Hill, and M. A. Pate, *Solid State Electron.* **31**, 707 (1988).

¹²A. Zaslavsky, D. C. Tsui, M. Santos, and M. Shayegan, *Phys. Rev. B* **40**, 9829 (1989).

¹³E. D. Jones, S. K. Lyo, I. J. Fritz, J. F. Klem, J. E. Schirber, C. P. Tigges, and T. J. Drummond, *Appl. Phys. Lett.* **54**, 2227 (1989).

¹⁴For a similar deduction of E_F in the contacts from the fundamental field at the peak of the resonance for 3D to 2D tunneling, but for a GaAs- $Al_xGa_{1-x}As$ -GaAs- $Al_xGa_{1-x}As$ structure, see Refs. 7 and 10.

¹⁵C. A. Payling, C. R. H. White, L. Eaves, E. S. Alves, M. L. Leadbeater, J. C. Portal, P. D. Hodson, D. J. Robbins, R. H. Wallis, J. I. Davis, and A. C. Marshall, *Superlatt. Microstruct.* **6**, 193 (1989).

¹⁶O. K. Kim and W. G. Spitzer, *J. Appl. Phys.* **50**, 4362 (1979).

¹⁷P. E. Simmonds, M. S. Skolnick, T. A. Fisher, K. J. Nash, and R. S. Smith, *Phys. Rev. B* **45**, 9497 (1992).